



Profilin (*pfn*) isoforms transcriptional and bioinformatic exploration and *Mus musculus* brain tissues development

Ammarah Fateen^a, Syed Aoun Ali^a, Deeba Noreen Baig^{a,*}, Zarrin Basharat^b

^a Department of Biological Science, Forman Christian College (A Chartered University), Zahoor Elahi Road, Lahore 54600, Pakistan

^b Department of Environmental Sciences, Fatima Jinnah Women University, 46000 Rawalpindi, Pakistan



ARTICLE INFO

Keywords:

Profilin

pfn1

pfn2

pfn3 and *pfn4*

ABSTRACT

Profilin (*pfn*) is an essential actin binding, post synaptic protein. Among its multiple isoforms, two (*pfn1* and *pfn2*) have been reported in various organs including brain. *pfn3* has been documented in kidneys and testes only, whereas *pfn4* exclusively in testes. In this study, we report the presence of *pfn* isoforms, *pfn3* and *pfn4* in *Mus musculus* brain in addition to *pfn1* and *pfn2*. Nine developmental stages were grouped into three classes, group 1: E10.5, E14.5, and E18.5 (prenatal), group 2: P0.5, P3.5, P5.5, P10.5 (postnatal) and group 3: P20.5, P60.5 (adult). Remarkably, all four isoforms exhibited variable yet significant expression in all discerning developmental stages. *pfn3* presented high levels of transcription while *pfn4* was transcribed minimally throughout all stages except P3.5. Computational prediction of these full length transcripts of *pfn* encoding genes reveals dynamic secondary structure and pseudoknots configurations. Conclusively, transcriptomic levels are greatly connected with compact base pairing association of their secondary structures. Codon usage bias of mRNA transcripts and string analysis were additionally carried out to analyze different attributes of *pfn* isoforms.

1. Introduction

Profilin (*pfn*) is an abundant, evolutionarily conserved, small (14–17 kDa) actin binding protein (ABP). It is involved in maintenance of cell integrity, motility and signal transduction. It has pivotal role in the remodeling of actin which is critical in organogenesis, healing of wounds, in immune responses, oocyte maturation, fertilization and embryonic development (Carlsson et al., 1977). *pfn1* has been evident control element in actin polymerization and cellular migration, *pfn1* gene disruption leads to abnormal growth and motility in single cells (Zhijie et al., 2012) and even leads to embryonic death in mammals (Witke et al., 2001). The three-dimensional structure of *pfn* isoforms are well conserved, comprised of a central seven-stranded β -sheet surrounded by the proximal N and C-terminal α -helices on one side and two short α -helices on the other side. It has two binding domains; one interacts with actin monomers and second interacts with the specific proline-rich motifs present in proteins (Bausen et al., 2006).

In eukaryotic cells *pfn*, splicing of *pfn* transcripts can generate many other variants of these isoforms (Lambrechts et al., 2000). *pfn1* express ubiquitously in almost all cell types, *pfn2* is a brain-specific isoform and its presence is crucial in neuronal development, whereas, *pfn3* and *pfn4* were reported only in testis and kidneys (Obermann et al., 2005). *Pfn2-synapsin-dynamin1* multiprotein complex induce neuronal excitability

which lead to alteration in behavior (Boyl et al., 2007). Whereas, *pfn3* and *pfn4* control testicular actin cytoskeleton dynamics and a proven factor in acrosome production and spermatid nuclear shaping (Obermann et al., 2005).

As a postsynaptic density protein, *pfn* has integral role in appropriate brain functioning. Neuronal network is mediated by post synaptic protein molecules and synapses to function within neuronal circuits. Thus, play pivotal role in synaptic plasticity and neuronal migration and tightly control development of synapse connections (Bourne and Harris, 2008).

One of the key features of neurogenesis is the migration of neurons from ventricular zone to neocortex. In rodent model (mice) at embryonic day 11.5 (E11.5), neurons generate pre-plate structure. The successive wave of neuronal migration at E13.5 divides pre-plate into two layers, first is superficial marginal zone, and second is deeper sub-plate (Ayala et al., 2007). Cerebral cortex development continues with subsequent waves of migration that locates neurons within separate layers in cortical plate. The correct positioning of neurons is responsible for appropriate brain functioning (Doetsch and Hen, 2005) suggesting the specific involvement of Pfn in neuronal migration during mammalian embryogenesis and a key candidate molecule in normal brain function.

On the other hand, Pfn, being an actin binding protein (ABP), is

* Corresponding author.

E-mail address: deebabaig@fccollege.edu.pk (D.N. Baig).

Table 1
Primer sequences for *gapdh*, *pfn1*, *pfn2*, *pfn3*, *pfn4* for PCR.

| Gene ID | Primer's sequences (5'–3') | Tm (°C) | Product size | Reference accession no. |
|-------------------|---|----------|--------------|-------------------------|
| <i>pfn1</i> | Forward = 5'-CCCCGAGCTCTCTGCCTT-3' Reverse = 5'-TATCTGTCCATCCAGCCCA-3' | 58 59 | 667 bp | NM_011072.4 |
| <i>pfn2</i> | Forward = 5'-AGTGCAGAGGGCTCGAAG-3' Reverse = 5'-CCCCTAATACTTAACAGTCTGCCTA-3' | 58 58 | 482 bp | NM_019410.3 |
| <i>pfn3</i> | Forward = 5'-AAGTTGCTGGGACTGACTGA-3' Reverse = 5'-GCACCCAGTTCACGGTTTAT-3' | 58 58 | 502 bp | NM_029303.2 |
| <i>pfn4</i> | Forward = 5'-ACTCCAGGAAAAGACCCTGT-3' Reverse = 5'-GTTGCTTCACTAGTTATCTTCGG-3' | 57 58 | 500 bp | NM_028376.3 |
| <i>gapdh</i> | Forward = 5'-CCCCTTCATTGACCTCAACTAC-3' Reverse = 5'-CCTTTTGGCTCCACCCCTT-3' | 58 57 | 250 bp | GU_214026.1 |
| <i>pfn1</i> (qRT) | Forward = 5'-GTGGAACGCCTACATCGAC-3' Reverse = 5'-TCAGCTGGCGTAATGCTAAC-3' | 59 59 | 132 bp | NM_011072.4 |
| <i>pfn2</i> (qRT) | Forward = 5'-GAGCATCACGCCAGTAGAAA-3' Reverse = 5'-TGACTCTTTGTCCGGATGTC-3' | 59 58 | 156 bp | NM_019410.3 |
| <i>pfn3</i> (qRT) | Forward = 5'-TGGAGGATCCTCAATAAGA-3' Reverse = 5'-TTTCAGAGCACCCAGTTCAC-3' | 58 58 | 131 bp | NM_029303.2 |
| <i>pfn4</i> (qRT) | Forward = 5'-CGAACACTTCTGAATGGATT-3' | 58 | 190 bp | NM_028376.3 |

involved in cytoskeletal dynamics. It binds with actin monomers and inhibits spontaneous assembly of actin polymers. Thus, expression of *pfn* is essential for proper neuronal translocation during brain development. Many genetic studies have revealed impaired neuronal migration is due to lack of *pfn* isoforms (Rust et al., 2012). However, no study has been undertaken till now which quantifies the expression of all these isoforms in murine brain at pre- and postnatal stages. Current study deals with the detection of *pfn1*, *pfn2*, *pfn3* and *pfn4* in the whole brain lysate of *Mus musculus*. Their differential expression levels were investigated at various pre and postnatal developmental stages (E10.5, E14.5, E18.5, P0.5, P3.5, P5.5, P10.5, and P20.5) to infer their status as crucial contributors in proper brain development and functioning.

2. Materials and methods

2.1. Ethics statement

The experimental procedures were carried out in compliance and accordance with Forman Christian College (A chartered University) Institutional Review Board's (FCCIRB) approved protocol. All efforts were made to minimize animal suffering.

2.2. Animal care

For *Mus musculus*, breeding and housing conditions were highly standardized, facilitating a reliable environment. Durable cages were used, resistant to heat and chemicals. Nutritionally adequate diet was provided to mice. Temperature was maintained at 24 °C, and humidity level was between 50 and 70%. Each pregnant mice housing was single and for postnatal mice, it was group housing. For postnatal (Group 2) and adult stages (Group 3), 3–4 female mice were sacrificed whereas for embryonic stages (Group 1), 9–10 pups were used for each stage and sex was not determined.

2.3. Brain surgery for tissue preparation

The day of vaginal plug detection was determined as first gestational day E 0.5. Embryonic E10.5, E14.5 and E18.5 stages were identified on the basis of plug date. Each Pregnant mice with specified embryonic days were anaesthetized by intraperitoneal injection of isoflurane (difluoromethoxy-1,1,1-trifluoro-ethane). Anaesthetized mother was operated and embryos were isolated in aqueous medium

(25 mM PBS) Whole embryonic brains were isolated immediately and quickly transferred in pre-chilled 500 µl TRIzol reagent (Sigma) according to manufacturer's instructions and homogenized at 4 °C. Homogenized brain tissues were stored at – 80 °C until further use.

2.4. RNA isolation and cDNA library synthesis

Total RNA was isolated from brain tissue at embryonic stages (Group 1: E10.5, E14.5 and E18.5), postnatal (Group 2: P0.5, P3.5, P5.5, P10.5) and adult stages (Group 3: P20.5 and P60.5) of wild type Swiss albino mice according to TRIzol® reagent (Sigma) manufacturer's instructions. Total RNA was treated with DNase 1 (Thermo Scientific) to remove genomic DNA and was dissolved in RNase free water. RNA concentration and purity were recorded by measuring the absorbance at 260 and 280 nm on NanoDrop (Thermo Scientific 2000c spectrophotometer). 2% agarose gel was used to further verify the presence of RNA. cDNA was synthesized from extracted RNA according to manufacturer's protocol (Thermo Scientific). Total RNA (1–10 µg), oligo (dT) primers (Thermo Scientific) and RNase free water were heated at 65 °C for 5 min to remove possible secondary structures, and immediately chilled on ice for 5 min. There-after, RT buffer (10 ×), dNTPs (10 mM), Ribolock, Revert aid RT and RNase free water (Thermo Scientific) were mixed gently and incubated at 42 °C for 60 min. The reaction mixture was heated at 70 °C for 10 min. Prior to use cDNA for gene amplification and qRT-PCR, it was diluted to 1:6 with RNase free H₂O.

2.5. Primer designing

Primers for qRT-PCR were designed using Genscript (<https://www.genscript.com/ssl-bin/app/primer>) (Table 1), on the terminal sequences of two consecutive exons in order to avoid binding of primers on the genomic DNA. For each gene three set of primers were used and best set was selected for all experiments with GAPDH as control.

2.6. Full length gene amplification of *pfn* isoforms

Full length gene amplification was carried out using gene specific primers for *pfn1*, *pfn2*, *pfn3* and *pfn4*. Reaction mixture were prepared by using diluted cDNA template, PCR buffer (10 ×), MgCl₂ (NH₂PO₄) (25 mM), dNTPs (2.5 mM) and *Taq* polymerase (1 U) (Thermo Scientific). Similarly Gene specific primers were designed for full length amplification of *pfn1*, *pfn2*, *pfn3*, *pfn4* gene by using web available

program Primer 3 and Primer BLAST (Table 1). Thermocycling conditions, denaturation at 94 °C, annealing at 58 °C, followed by extension step at 72 °C. Amplified products were resolved on 1.2% agarose gel and data was recorded in gel documentation system (GelDoc-It 310 imaging system).

2.7. DNA sequence analysis

RT-PCR product was purified according to manufacture instructions (Favorgen). Purified PCR product samples were stored at –20 °C. Sanger Sequencing was done by Commercially available services (Eurofins) forward and reverse primers for *pfn1*, *pfn2*, *pfn3* and *pfn4*. Sequences were aligned and analyzed by Blast in NCBI.

2.8. Secondary structure analysis of profilin isoforms

RNA Secondary structures of *pfn* mRNA sequences were computed by using NUPACK RNA analysis software (www.nupack.org) by Caltech, California USA (Dirks and Pierce, 2004) (Zadeh et al., 2011, b). Pseudoknots configurations of coding transcript were obtained using web available Probknot server (<http://rna.urmc.rochester.edu/>) developed and maintained by Mathews Labs at University of Rochester Medical Center. For the evaluation of the predicted pseudoknots, pairs were found using algorithm and each base pair is calculated accordingly (Reuter and Mathews, 2010).

2.9. Differential transcription analysis of genes (qRT-PCR)

GenScript Real-time PCR (TaqMan) Primer Design (<https://www.genscript.com/ssl-bin/app/primer>) was used to design qPCR primers sets for *pfn1*, *pfn2*, *pfn3* and *pfn4* isoforms and GAPDH. The qPCR analysis was performed in CFX96 Real-Time PCR (Bio–Rad) using SYBR Green I mixture in a final volume of 15 µl. 1 µg of total RNA was used for cDNA synthesis which was diluted 6 × for transcriptional analyses of profilin isoforms (*pfn1*, *pfn2*, *pfn3*, *pfn4*) in prenatal, postnatal and adult brain samples by using qRT-PCR. For each 15 µl reaction mixture was comprises SYBR Green I mix (Life technologies, Thermo Fisher Scientific, USA), 0.75 µl forward primer (10 µM) and 0.75 µl reverse primers (10 µM), cDNA (1 µl) and RNase free water. GAPDH (housekeeping gene) was used as an internal control in all q-PCR experiments.

qPCR thermocycling conditions include initial denaturation at 94 °C for 3 min, followed by 35 cycles of denaturation at 94 °C for 45 s whereas annealing temperature was set at 57 °C for 6 s which was followed by extension at 72 °C for 1 min. All experiments were conducted in triplicates. Melt curve analysis was recorded and analyzed the specificity of the reaction.

2.10. Statistical analysis

Data were analyzed for significance by one-way analysis of variance (ANOVA) followed by post-hoc Tukey's multiple comparison tests to check variability in the expression levels. *P* value < 0.05 was considered as significant (*P* < 0.05).

3. Results

3.1. Sequence analysis

pfn1, *pfn2*, *pfn3* and *pfn4* complete coding transcripts were amplified from selective developmental stages. Amplified product size of 667 bp, 482 bp, 502 bp and 500 bp were observed respectively (Fig. 1). Sanger sequencing confirmed the sequences of desired genes (*pfn1*, *pfn2*, *pfn3*, *pfn4*). Nucleotide BLAST (BLASTn) analysis showed the 100%

(NM_011072.4) and 99% (NM_019410.3) identity of *pfn1* and *pfn2* sequences respectively. *Pfn3* and *pfn4* gene sequences showed 100% (NM_029303.2) and 99% (NM_028376.3) sequence identity with reference sequences mentioned in Supplementary Table 1.

3.2. RNA secondary structure analysis

NUPACK online server (MIT, USA) was used for *pfn*'s RNA secondary structures prediction. Fig. 2 encompasses un-pseudoknotted targeted structure with minimum free energy (MFE). The most stable structural free energies for *pfn1*, *pfn2*, *pfn3* and *pfn4*, –165.72 kcal/mol, –85.60 kcal/mol, –166.80 kcal/mol and –98.20 kcal/mol respectively (Supplementary Table 2).

Pfn's transcripts secondary structures were extensively variable in folding configurations which exhibits distinct loops and branches. The concise mRNA structure of *pfn 1* highlights typical one sided folded structure, *pfn 2*mRNA reveals relatively linearized with least folded patterns. *pfn 3* transcript although is extensively branched with minimum complementarity. However, the *pfn 4* transcript is unique in its secondary structure which displays maximum complementary region in variable number of numerous branches. These predicated secondary structures folds' reveals enable us to explain the pseudoknots pattern in Fig. 3.

3.3. Pseudoknots

For each mRNA sequence of *pfn*, pseudoknots were predicted using ProbKnot online server. In Fig. 3, ProbKnot algorithm predicts *pfn* mRNA sequence on the bases of most probable base pairing within their sequences and with themselves. Each pseudoknot based mRNA transcript configuration represents probable base pairing for each member of *pfn* which reflects in remarkable dissimilarities. *Pfn 1* and *pfn 3* presented non-pseudoknots structure whereas *Pfn 2* and *pfn 4* have dynamic form of pseudoknots patterns extending throughout their transcripts. *Pfn 2* however showed distant complementary base pairing whereas *pfn 4* signifies constricted pairing with minimally exposing the transcript structure. These dynamic pseudoknots configurations contribute towards active expression of different *pfn* isoforms.

3.4. Transcriptional analysis

Among embryonic stages, *pfn1* had highest expression at E18.5 stage, followed by E10.5 which showed slightly lower expression than E18.5 and at E14.5, expression was lower than E10.5 and E18.5. *pfn2* showed equal and highly significant expression at E18.5 and E14.5 and minimum at E10.5. *pfn3* was highly expressed at E10.5 and E18.5, whereas, lower at E14.5. *pfn4* showed low expression at embryonic stages but it was significant at E18.5 compared to E10.5 and E14.5. Among postnatal stages, *pfn1* had highest expression at P0.5, it became slightly lower at P10.5 and at P20.5, P3.5, P5.5 and P60.5 expression was uniform and lower than P0.5, P10.5 and P20.5. *pfn2* had equal and highly significant expression at all postnatal stages. *pfn3* was highly expressed at P60.5 then at P0.5 and P5.5, at P10.5 and P20.5 it was expressed at equal level slightly lower than P60.5 and P0.5. *pfn4* showed highest expression at P3.5 then at P10.5 and P20.5. P5.5 and P60.5 had very low expression equal to embryonic stages E10.5 and E14.5. These results reveal almost consistent expression of *pfn2* throughout all stages whereas other isoforms have variable expression, however, *pfn4* exhibited extremely down regulated state in transcription. Detection and identification of these isoforms in brain at significant level suggests them as vital in brain development.

One-way ANOVA followed by Post-hoc Tukey's HSD multiple comparison tests for all of the three groups showed highly significant difference in overall expression level of *pfn* isoforms and *gapdh*

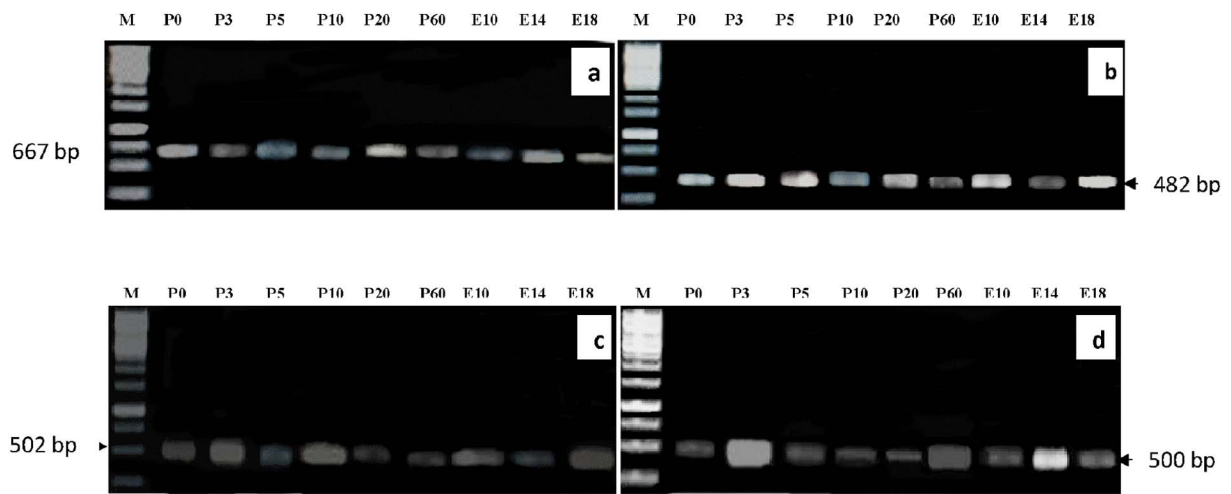


Fig. 1. Full length mRNA coding transcript amplification, M: DNA marker (Thermo Scientific, SM 0311) (a) *pfn1* with the size of 667 bp in brain of *Mus musculus* (b) *pfn2* (482 bp) in brain of *Mus musculus* (c) *pfn3* (502 bp) in brain of *Mus musculus* (d) *pfn4* (500 bp) in brain of *Mus musculus*.

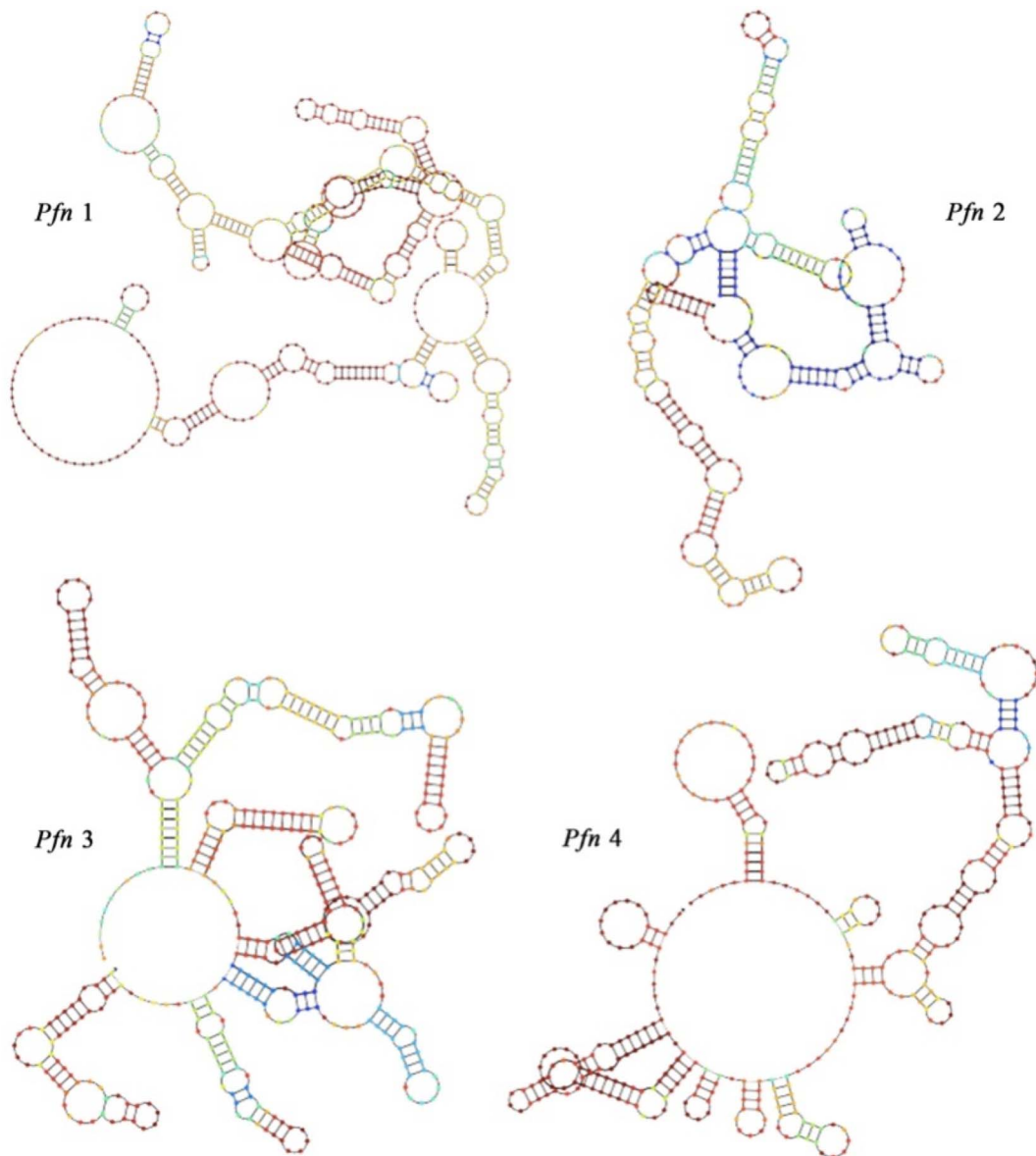


Fig. 2. *pfn*'s mRNA transcript secondary structures predictions.

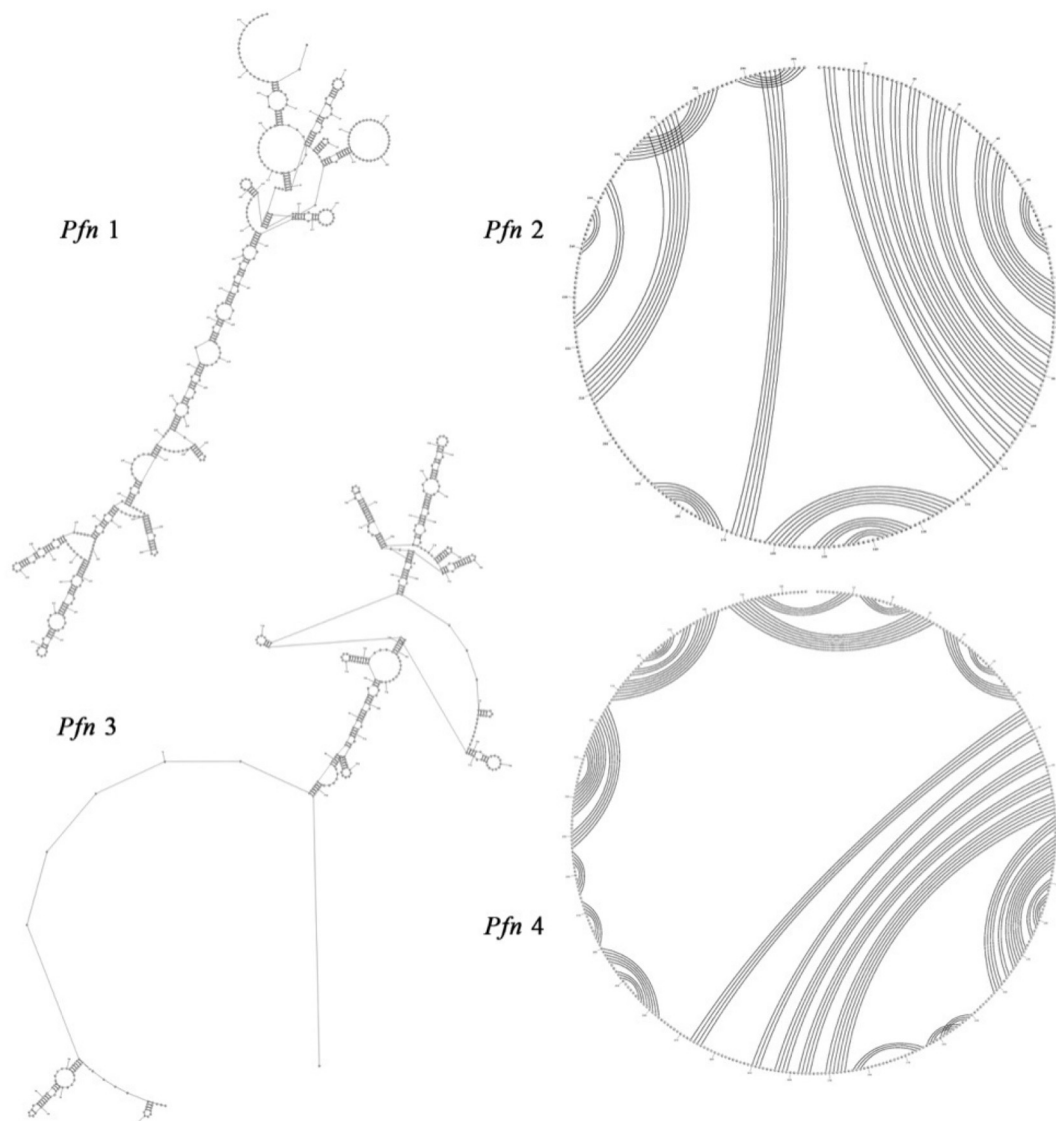


Fig. 3. Pseudoknots prediction for *pfn*'s mRNA sequences.

($P < 0.05$). *pfn4* exhibited highly different expression at all of the nine developmental stages in comparison with *gapdh*, *pfn1*, *pfn2*, *pfn3* (Supplementary Table 3).

4. Discussion

In reference of *Pfn(s)*, there is a strong interaction with synapsin and dynamin during neuronal excitability, which ultimately leads to altered behavior (Boyl et al., 2007). Later on Birbach (2008) explained the *Pfn* (s) as essential elements in morphology of dendrites and spines and equally important in neuronal plasticity during developmental processes. Among all isoforms of *pfn*, *pfn1* and *pfn2* are well reported actin polymerization partners in neurogenesis stages. However, least is known about the expression of *pfn3* and *pfn4* during different developmental stages. Our previously published report revealed the prevalence of *pfn3* in the rodents brain (Tariq et al., 2016), which directed us to explore the expression profile of *pfn4* during different developmental stages of brain. In our current study, all isoforms of *pfn* family were detected in the brain. However, transcriptional expression is highly variable in all stages. *Pfn2* was most prevalent and frequently expressed isoform during whole developmental process. In contrast to *pfn2*, the

transcriptional levels of *pfn1* are relatively lower in most of the selected stages except were in E18.5. On the other hand the transcription of *pfn3* is significantly up-regulated during same stage (E10.5, E18.5 and P3.5), Whereas, *pfn4* is predominantly down regulated throughout the brain development, except P3.5. The reason of high expression of *pfn4* in a specific developmental stage needed to be explored. Present study is inculcating new data on the prevalence of *pfn4* in the brain cells, which was only reported in the testis so far. The downregulation of *pfn4* during developments profile is a question mark for the future studies (Fig. 4).

Significantly high levels of *pfn1* in brain at embryonic stages suggests critical role of this isoform during brain processing which is in positive co-relation of Witke et al. (2001) which reveals that *pfn1* deficient mouse die during very early development because it has dosage dependent effect on cell division and survival of embryos. Presence of *pfn1* in postnatal stages is in parallel to Kullman et al. reports (2011) which showed that inactivation of *pfn1* during brain development of adults can impede neuronal migration. These evidences proven the fact that *pfn1* at prenatal and postnatal stages are transcribed in variable levels.

Jockusch et al. (2007), explained predominant neuronal expression

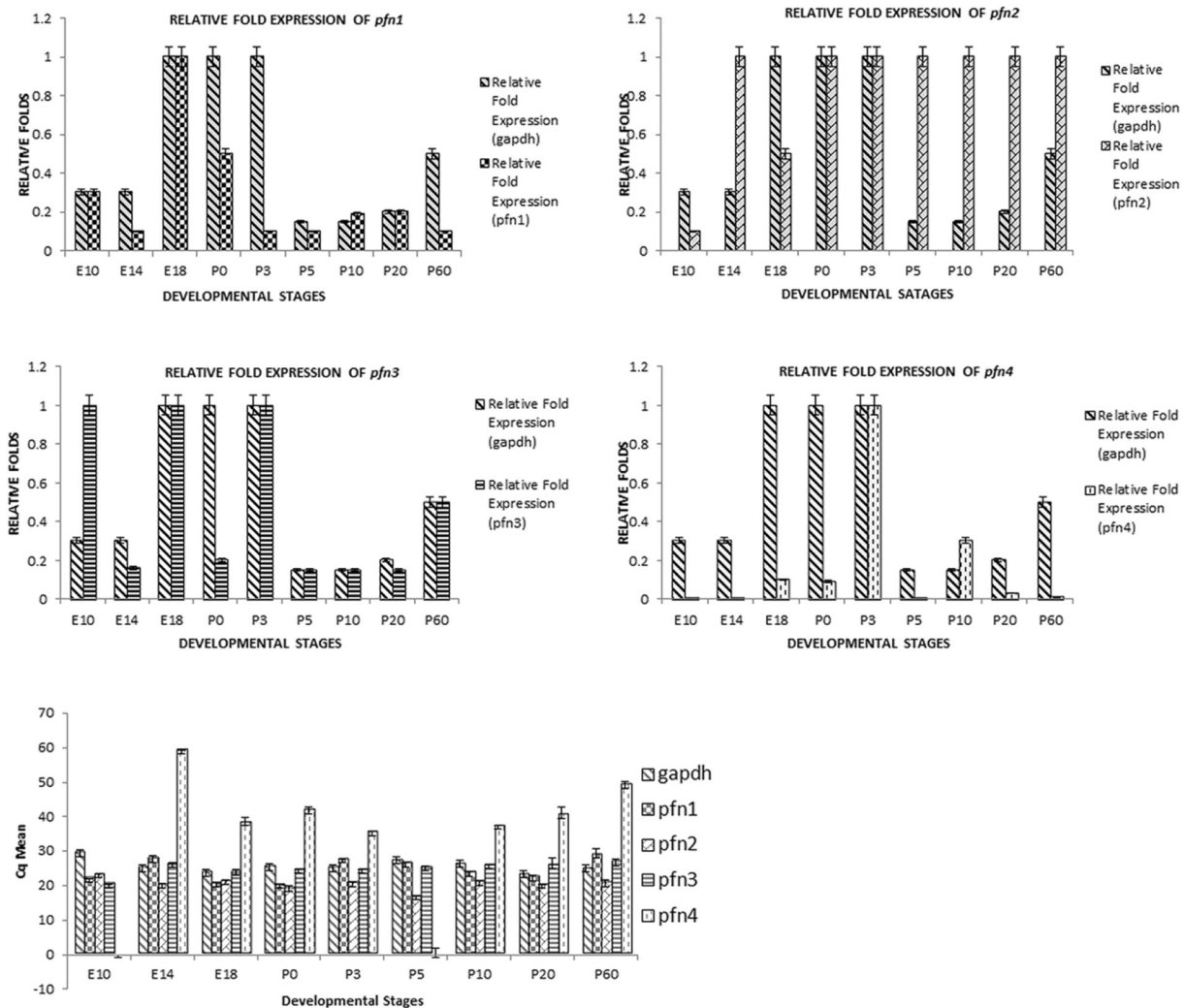


Fig. 4. Transcriptional analysis of *pfn* 1, 2, 3 and 4 in developmental stages (E10.5, E14.5, E18.5, P0.5, P3.5, P5.5, P10.5, P20.5, P60.5).

of *pfn2* throughout the development, which provide support to the present data with significantly high expression in E14.5, P0.5, P3.5, P5.5, P10.5, P20.5 and P60.5 stages. High expression level of *pfn2* in E14.5 (embryonic day 14) brain equal to postnatal and adult stages indicates that *pfn2* is required in more quantity at E14.5 embryonic stage because there is development of different brain layers at this specific stage. Similarly, *pfn2* plays important role in neuronal migration of neurons from lateral ventricles to the pial surface of brain. Thus, transcriptional expression reveals that *pfn2* is critically essential molecule in normal neurogenesis including spine morphology and complexity of dendrites (Michaelsen et al., 2010). The variable transcriptional efficiency of *pfn3* and *pfn4* suggested their involvement in specific brain development process. The expressional profile of both newly identified isoforms needed to be co-related with different brain developmental mechanisms.

Detection and identification of *pfn3* and *pfn4* in brain at prenatal, postnatal and adult stages of mouse implicate them as potential partners of other *pfn* isoforms sharing some common pathways involved in the process of neurogenesis along with the spermatogenesis. Therefore, it is highly critical to explore the functions of *pfn3* and *pfn4* in various neuronal processes. In this study, a model for molecular interactions of *pfn3* and *pfn4* has been proposed by which they contact with different molecular partners involved both in neurogenesis and spermatogenesis. Possible molecular interactions of *pfn3* and *pfn4* have been shown in

Fig. 5, all these interactions involved in neurogenesis and spermatogenesis are based on data from literary studies which represent that in order for the newly divided neurons, extracellular guidance cues, growth factors, neurotrophic factors, and cell adhesion complexes trigger a wide range of intracellular signaling pathways to approach their correct position. Both neurons and sperms have high concentrations of PUFAs (polyunsaturated fatty acids) relative to other body tissues. In neurons, fatty acids are concentrated at synaptic terminals and play a central role in neurodevelopment function and maintenance by interacting with different proteins involved in sodium and calcium depolarization. Thus, controlling synaptic plasticity and also regulating the sperm metabolism during spermatogenesis. *pfn3* and *pfn4* interact with different molecules involved in neurogenesis and spermatogenesis, triggering a broad range of intracellular signaling cascades and pathways ultimately ending in the coordinated regulation of cytoskeletal dynamics in neurons and sperms.

5. Conclusions

This study presents the identification and differential transcriptional expression of *pfn* isoforms (*pfn1*, *pfn2*, *pfn3* and *pfn4*) at pre and post embryonic stages of *Mus musculus*. Furthermore, the identification of *pfn3* and *pfn4* provides the primary basis for further investigation of their role in mammalian brain development.

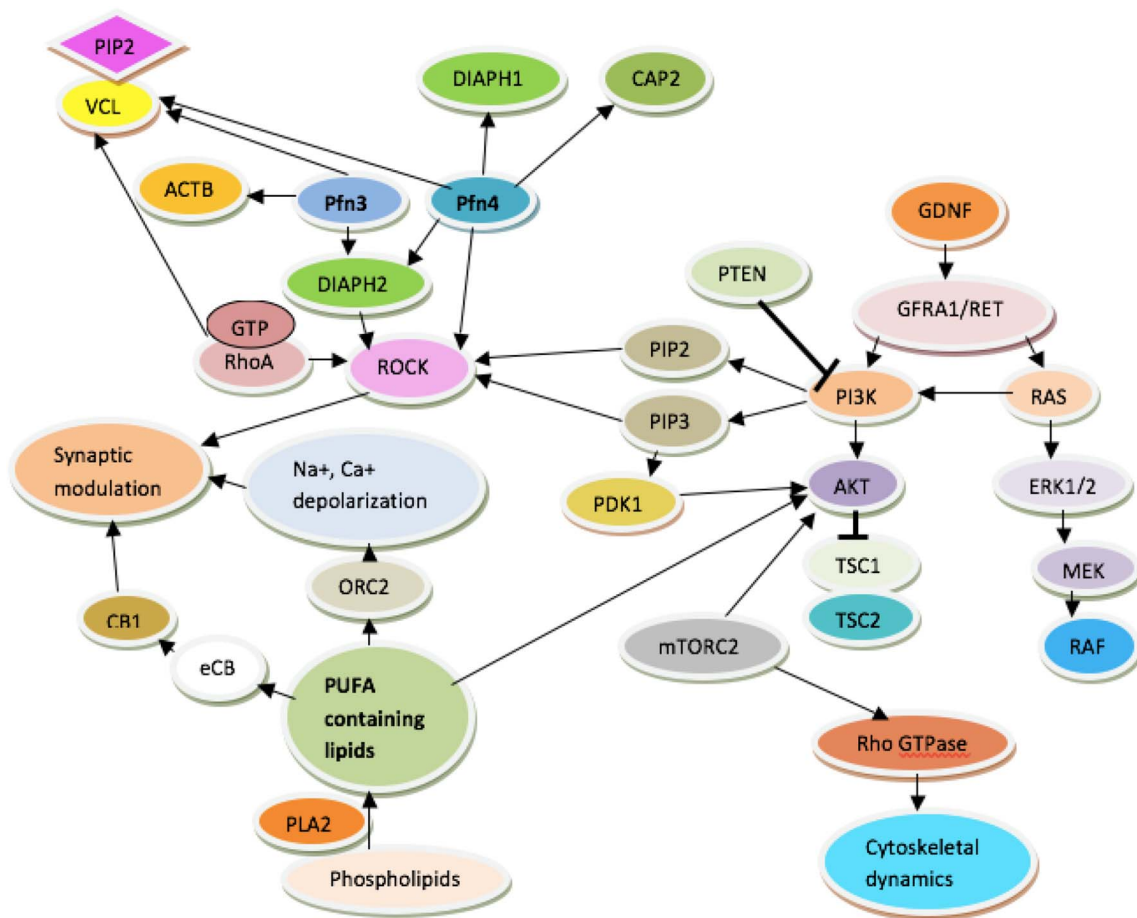


Fig. 5. Proposed model for molecular interactions of *pfn3* and *pfn4* involved in neurogenesis and spermatogenesis.

Acknowledgment

The authors are thankful to Dr. Muhammad Ali, School of Biological Sciences, University of Punjab, Lahore, Pakistan, for providing support in animal breeding. The study was conducted on the funds of Department of Biological Sciences, Forman Christian College (A Chartered University). No external funding or grants were utilized for the experimental work and publication.

Appendix A. Supplementary data

Supplementary data to this article can be found online at <https://doi.org/10.1016/j.genrep.2017.12.005>.

References

Ayala, R., Shu, T., Tsai, L.H., 2007. Trekking across the brain: the journey of neuronal migration. *Cell* 12, 10–1016.
 Bausen, M., Fuhrmann, J.C., Betz, H., O'Sullivan, G.A., 2006. The state of the actin cytoskeleton determines its association with gephyrin: role of ena/VASP family members. *Mol. Cell. Neurosci.* 31, 376–386.
 Birbach, A., 2008. Profilin, a multi-modal regulator of neuronal plasticity. *BioEssays* 30, 994–1002.
 Bourne, J.N., Harris, K.M., 2008. Balancing structure and function at hippocampal dendritic spines. *Annu. Rev. Neurosci.* 31, 47–67.
 Boyd, P.P., Di Nardo, A., Mulle, C., Sassoe-Pognetto, M., Panzanelli, P., 2007. Profilin2 contributes to synaptic vesicle exocytosis, neuronal excitability, and novelty-seeking behavior. *EMBO J.* 26, 2991–3002.
 Carlsson, L., Nyström, L.E., Sundkvist, I., Markey, F., Lindberg, U., 1977. Actin polymerization is influenced by profilin, a low molecular weight protein in non-muscle

cells. *J. Mol. Biol.* 115, 465–483.
 Dirks, R.M., Pierce, N.A., 2004. An algorithm for computing nucleic acid base-pairing probabilities including pseudoknots. *J. Comput. Chem.* 25, 1295–1304.
 Doetsch, F., Hen, R., 2005. Young and excitable: the function of new neurons in the adult mammalian brain. *Curr. Opin. Neurobiol.* 15, 121–128.
 Jockusch, B.M., Murk, K., Rothkegel, M., 2007. The profile of profilins. *Rev. Physiol. Biochem. Pharmacol.* 159, 131–149.
 Lambrechts, A., Braun, A., Jonckheere, V., Aszodi, A., et al., 2000. Profilin II is alternatively spliced, resulting in profilin isoforms that are differentially expressed and have distinct biochemical properties. *Mol. Cell. Biol.* 20, 8209–8219.
 Michaelsen, K., Murk, K., Zagrebelsky, M., Dreznjak, A., Jockusch, B.M., 2010. Fine-tuning of neuronal architecture requires two profilin isoforms. *Proc. Natl. Acad. Sci. U. S. A.* 107, 15780–15785.
 Obermann, H., Raabe, I., Balvers, M., Brunswig, B., et al., 2005. Novel testis-expressed profilin IV associated with acrosome biogenesis and spermatid elongation. *Mol. Hum. Reprod.* 11, 53–64.
 Reuter, J.S., Mathews, D.H., 2010. RNAstructure: software for RNA secondary structure prediction and analysis. *BMC Bioinformatics.* 11, 129.
 Rust, M.B., Kullman, J.A., Witke, W., 2012. Role of the actin-binding protein profilin1 in radial migration and glial cell adhesion of granule neurons in the cerebellum. *Cell Adhes. Migr.* 6, 13–17.
 Tariq, N., Basharat, Z., Butt, S., Baig, D.N., 2016. Distribution analysis of Profilin isoforms at transcript resolution with mRNA-seq and secondary structure in various organs of *Rattus norvegicus*. *Gene* (589), 49–55.
 Witke, W., Sutherland, J.D., Sharpe, A., Arai, M., Kwiatkowski, D.J., 2001. Profilin I is essential for cell survival and cell division in early mouse development. *Proc. Natl. Acad. Sci. U. S. A.* 98, 3832–3836.
 Zadeh, J.N., Steenberg, C.D., Bois, J.S., Wolfe, B.R., Pierce, M.B., Khan, A.R., Dirks, R.M., Pierce, N.A., 2011. NUPACK: analysis and design of nucleic acid systems. *J. Comput. Chem.* 32, 170–173.
 Zadeh, J.N., Wolfe, B.R., Pierce, N.A., 2011. Nucleic acid sequence design via efficient ensemble defect optimization. *J. Comput. Chem.* 32, 439–452.
 Zhijie, D., Yong, H.B., Partha, R., 2012. Molecular insights on context-specific role of profilin-1 in cell migration. *Cell Adhes. Migr.* 6, 442–449.